Energy Performances Analysis of a Solar Electric Car in Togo

Kokou Prosper Semekonawo [a*] and Sié Kam [a]

[a] *Université Joseph KI-ZERBO, 03 BP 7021 Ouagadougou 03, Laboratoire d'Energies Thermiques Renouvelables, Ouagadougou, Burkina Faso.*

Authors' contributions

This work was carried out in collaboration between both authors. Both authors read and approved the final manuscript.

Original Research Article

ABSTRACT

In sub-Saharan Africa the cost of transport is very expensive for the populations. As the car fleet is mainly made up of thermal cars, the high cost of transport is largely linked to the oil's import. Faced with such a situation, it is important to find other means of transport in order to reduce the transport's cost for the populations. One of the means of transport which seems to be an alternative solution is the solar electric car. But the difficulty for the solar electric car is its range. To improve car's range, it is necessary to analyze the performance of the car in driving conditions in order to understand the parameters that influence the range. Understanding and mastering these parameters will make it possible to make the best decisions to improve the car's range. In this article, we are interested in analyzing the energy performances of a solar electric car in Togo in order to understand the parameters that influence the car's range. The simulation results show a considerable reduction in the car's range for high driving speeds, for excessive consumption of the auxiliary electrical circuits of the car, for driving the vehicle on a large slope, and when the car is transporting a large weight. The solar panel on the roof of the car is of great importance because it makes a significant contribution to the car's range in sunny periods.

Keywords: Car's range; energy; performance; solar electric car.

_____

*Corresponding author: E-mail: prospersem01@gmail.com;

ABREVIATIONS

Designation and units used in the study:

Designation	Meaning	Units
Cm	Engine couple	N.m
Co	Battery capacity	Ah
CRRmoy	Rolling resistance coefficient	-
CT	Total capacity	Ah
Cu	Useful motor torque	N.m
Ec	Energy consumed	Wh
Ep	Energy produced	Wh
ET	Total energy	Wh
FF	Form factor	-
g	Gravity	N/kg
G	Solar radiation	W/m²
Icc	short circuit current	A
Ipm	Optimal current	A
Ireg	Regulator intensity	A
M	Mass	kg
η	Yield	-
p%	Slope	-
Pc	Peak power	Wp
Pdispo	Panel power available	Wp
PT	Total power	W
Pu	Useful power	W
S	Surface	m^2
Smin	Minimum cable section	mm²
V	Battery voltage	V
Vco	Open circuit voltage	V
Vpm	Optimal tension	V
Vvéh	Vehicle speed	km/h
Ω	Rotation speed	rd/s

1. INTRODUCTION

Togo, like most countries in sub-Saharan Africa, depends on oil imports to meet the needs of a growing vehicle fleet. In 2018, the transport sector was estimated to cover 15% of the overall consumption of Sub-Saharan Africa's energy system [1]. In the case of Togo, the transport sector represented 13.2% of the consumption of the energy system in 2016 [2]. Over the period 2010 to 2015, there was an annual growth of 10% for 2-wheel vehicles and 12% for 4-wheel vehicles [3]. Nevertheless, faced with this oil's price increase opposed the low purchasing power of the populations. The direct consequences of this are the high cost of transport, the inability of populations, especially those living in rural areas, to have access to means of transport and the pollution increase in the transport sector.

It is important to find solutions to this. The solution that seems sustainable, especially in this globally context of climate change, is the solar electric car. This solution provides many benefits for the populations in terms of independence from oil's cost fluctuations, reduction in vehicle maintenance costs, reduction in atmospheric and noise pollution, etc. [4-7].

But what can be the performance of such a technology (solar electric car)? Is this technology capable of satisfying populations in term of mechanical and range's performance like the thermal vehicle? How does the performance of such technology evolve in a Togolese and sub-Saharan context?

Edwin et al. [8] present an approach allowing to compare the energy consumption of an electric vehicle (EV) in different maneuvers of driving scenarios. The results of their study shows that reducing driver aggressiveness on accelerations is the main factor in reducing EV consumption in urban settings.

Martin et al. in [9] show that the vehicle weight and battery pack size have a main impact on the range. Their results conclude that vehicle weight increases directly with battery capacity. In the case that the electric vehicle has high capacity battery pack and is used for short distances for example EV with 24 kWh battery pack for 70 km range the vehicle is less efficient than the same vehicle with 8 kWh battery pack.

Apart from battery capacity, battery temperature, the overall vehicle driving environment and driver behavior are also factors that influence the range of electric vehicles [10]. The driving environment such as freezing temperatures and strong winds drastically reduce vehicle's range. In [11] Skuza and Jurecki show that negative temperatures can reduce EV's range by up to 37%, while at a temperature of 40°C, it is possible to extend the range by about 2%.

2. MATERIALS AND METHODS

2.1 General Presentation of the Solar Electric Car (SEC) Power System

The solar electric vehicle on which our study relates is composed of an electric motor mounted on the rear axle, a battery pack, voltage converters, calculators, a capacitor, a photovoltaic panel and a charge regulator. The technical characteristics of the SEC is:

- Aluminum profile structure
- A net weight of 395 kg
- Dimensions: 2930mm×1360mm×1550mm
- 60V/2200W Brushless motor
- A 60V/130 Ah battery pack
- Wheels: 135/70 R12
- Speed: 40-45km/h
- Range: 180 km

2.2 Longitudinal Dynamics Model of the SEC

When the vehicle is moving on a road with a slope p%, it is subjected to several forces, the balance of which is shown in Fig. 2.

The traction force F_t between the tires of the driving wheels and the road surface is produced by the engine torque and makes it possible to propel the vehicle forward. Nevertheless, resisting forces prevent the advance of the vehicle. These resisting forces include rolling resistance, aerodynamic drag and uphill resistance.
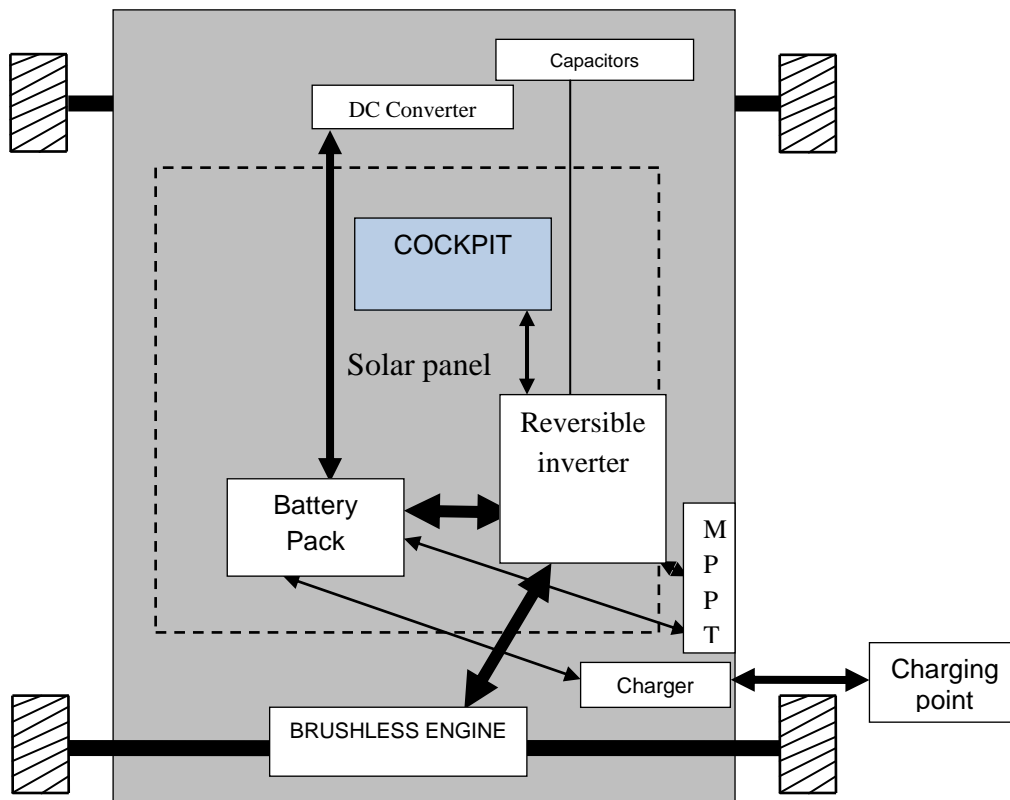

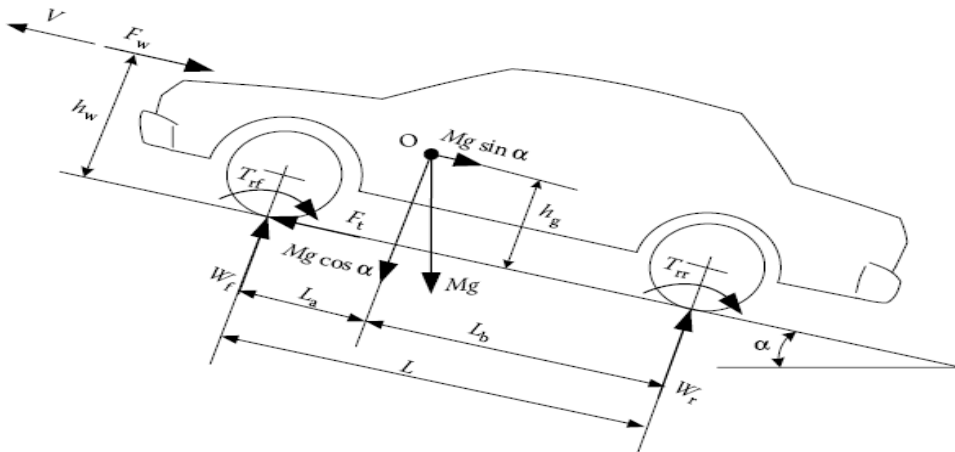**Fig. 1. General presentation of the SEC power system**

Fig. 2. SEC's longitudinal dynamics model

Thus, by applying the fundamental principle of dynamics to the vehicle, we obtain the relation (1).

$$M \, {}^{\mathrm{dv}}/_{dt} = \left(F_{tf} + F_{tr}\right) - \left(F_{rf} + F_{rr} + F_g + F_w\right) \quad (1)$$

F_{rf} and F_{rr} represent the rolling resistances of the front and rear tires. They are represented in relation Eq.2 by the Froul force.

F_{tf} and F_{tr} represent the tractive effort of the front and rear tires. They are represented in relation (2) by the force Fr.

F_w represents the aerodynamic drag, F_g the resistance of the slope, M the total weight of the vehicle (load in the vehicle included).

${}^{dv}/_{dt}$ represents the acceleration of the vehicle. It is represented in relation (2) by ɣ. Its value is positive (ɣ > 0) for acceleration and negative (ɣ < 0) for deceleration.

The traction force that the vehicle must therefore develop for its forward movement is given by the equation (2).

$$F_r = F_{roul} + F_w + F_g + M\gamma \quad (2)$$

The tensile force is:

$$F_r = {}^{(c_r)roues}/_{R_r} \quad (3)$$

The rolling resistance force is:

$$F_{roul} = CRR_{moy} \times M \times g \quad (4)$$

The aerodynamic drag force is:

$$F_w = {}^{1}/_{2} \times \rho \times S_f \times C_x \times V_{v\acute{e}h}^2 \quad (5)$$

The slope resistance force is:

$$F_g = M \times g \times sin\alpha = M \times g \times p\% \quad (6)$$

.

Thus, the relation Eq.2 can be rewritten as follows:

$$(Cr)_{roues} = (CRR_{moy} \times M \times g + {}^{1}/_{2} \times \rho \times S_f \times C_x \times V_{v\acute{e}h}^2 + M \times g \times p\% + M\gamma) \times R_r \quad (7)$$

In this last equation, (C_r)wheels represents the resistive torque applied to the wheels, CRR_{moy} the coefficient of rolling resistance, g the gravity, ρ the density of the air, Sf the frontal section of the vehicle, C_x the coefficient of penetration in the air, V_{veh} the speed of the vehicle and R_r the radius of the wheel.

(C_r)wheels being the resistive torque applied to the wheels, it is delivered by the electric motor (C_m) through a mechanical transmission with reduction ratio (n). Thus, the electromagnetic torque delivered by the motor to allow the vehicle to move forward is therefore given by the following equation:

$$C_m = (CRR_{moy} \times M \times g + {}^{1}/_{2} \times \rho \times S_f \times C_x \times V_{v\acute{e}h}^2 + M \times g \times p\% + M\gamma) \times {}^{R_r}/_{n} \quad (8)$$

2.3 Mathematical Modeling of Power System Elements

2.3.1 The photovoltaic solar panel

It comes from the association in a matrix of photovoltaic cells and makes it possible to produce electricity in the presence of light

(photonic energy). The main element of a photovoltaic panel is the photovoltaic cell.

A photovoltaic cell consists of a junction of two extrinsic semiconductors creating a pn junction. In the presence of light, the electrons are expelled from the atoms and we observe the appearance of electron-hole pairs within the material. Subjected to the electric field of the junction, these electron-hole pairs are separated and this leads to the storage of electrons and holes on either side of the junction. The appearance of a pdp is therefore observed at the terminals of the cell. Connected to an external circuit, it provides an electric current proportional to the amount of solar radiation received. Electrically, the photovoltaic cell is a diode which makes it possible to produce electric current in the presence of light [12].

The characteristic equation of the photovoltaic cell is therefore given by:

$$I = Iph - Is\left[\exp\left(\frac{q(V + Rs \times I)}{nkT}\right) - 1\right] - \frac{V + Rs \times I}{Rsh} \tag{9}$$

Thus for a surface S of the panel, we have a yield of the panel given by:

$$\eta = (Vpm \times Ipm)/(S \times G) \tag{10}$$

2.3.2 The Brushless engine

Being an electric motor, it produces mechanical energy thanks to the electrical energy it receives. It is a stator made up of three phase-shifted windings by an angle of 120° (powered by three-phase alternating currents), a rotor with permanent magnets and Hall effect sensors making it possible to permanently identify the position of the rotor. Its operating principle is that of a synchronous motor whose angle (θ) between the rotor field and the stator field is

permanently adjusted to the maximum (θ = π /2) in order to guarantee maximum motor torque and avoid the phenomenon of engine stall.

Thus, the origin of its name (autopilot synchronous motor) comes from the automatic piloting of the rotor by the reversible Converter-Hall effect sensors assembly. This system is also called brushless direct current motor in reference to the function of the commutators and brushes of the classic direct current motor [13].

Consisting of p pairs of poles and the rotor rotating in synchronism with the rotating stator field at the angular speed ω, then the speed of the motor Ω can be written as follows:

$$\begin{cases} \Omega(rd/s) = \frac{\omega}{p} = \frac{2 \times \pi \times f}{p} \\ n\ (tr/s) = \frac{f}{p} \end{cases} \tag{11}$$

Depending on the electrical model, we could write:

$$\underline{V} = \underline{E} + (R + jX) \times \underline{I} \tag{12}$$

Fresnel frame and by considering a steady state, we deduce the following relations:

$$\begin{cases} E = K \times N \times f \times \emptyset \\ P = 3 \times V \times I \times \cos\varphi \\ Pem = 3 \times E \times I \times \cos\psi = P + 3 \times R \times I^2 \\ Pj = 3 \times Rs \times I^2 \end{cases} \tag{13}$$

And so, we can determine the different expressions of the torque of the motor:

$$\begin{cases} Cm = \frac{P}{\Omega} = \frac{3 \times V \times I \times \cos\varphi}{\Omega} = \frac{3 \times p \times V \times I \times \cos\varphi}{\omega} \\ Cm = \frac{3 \times p \times E \times I \times \cos\psi}{\omega} \\ Cm = \frac{3 \times p \times V \times E \times \sin\theta}{L \times \omega^2} \end{cases} \tag{14}$$
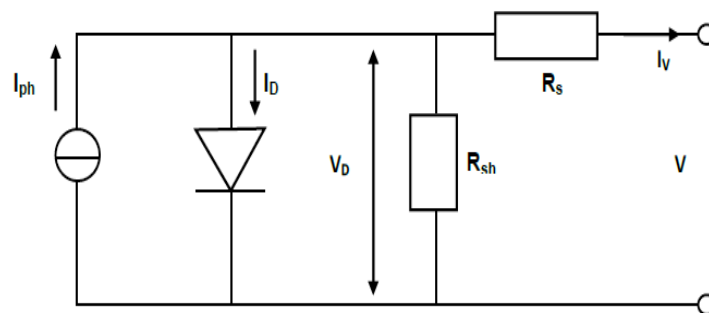

Fig. 3. Electrical model of a PV solar cell

We therefore deduce the expression of efficiency in motor mode, as well as in generator mode (during regenerative braking or during deceleration):

$$\begin{cases} \eta = \frac{\sqrt{3} \times U \times I \times cos\varphi - Pc - Pj}{\sqrt{3} \times U \times I \times cos\varphi} = \frac{Cu \times \Omega}{Cu \times \Omega + Pj + Pc} \; (Moteur) \\ \eta = \frac{\sqrt{3} \times U \times I \times cos\varphi}{U \times I \times cos\varphi + Pj + Pc} \; (Alternateur) \end{cases}$$

(15)

In these different expressions, f represents the frequency of the power supply network, E the electromotive force per winding, constant of Kapp (depending on the motor), N the number of conductors in a winding, $\emptyset$ the maximum flux passing through a turn, P the electrical power of the motor, V the phase-to-neutral voltage at the terminals of a winding, I the current flowing per phase of the stator, φ the phase difference between current and voltage, Pem the electromechanical power of the motor, ψ the angle between E and I, Pj thermal losses in the stator windings, Rs the resistance per stator winding, Cm electromechanical torque of the motor, Cu useful torque of the motor and Pc the constant losses of the motor (Pc is also the sum of the iron losses and the mechanical losses of the motor).

2.3.3 Reversible converter

Playing the role of frequency regulator and voltage inverter, it works in conjunction with Hall effect sensors. The sensors send impulses to the converter about the position of the motor rotor, the speed of rotation and the temperature of the motor.

The operation of the converter can therefore be modeled as a three-phase inverter with Pulse Width Modulation (PWM) control operating in two directions (possibility of recharging the battery when the motor is running in alternator) [14].

Thus, pulses of variation of the input voltage of the inverter lead to a variation of the output frequency of the converter making it possible to control the motor in speed.

A three-phase inverter is an electronic device used to convert direct voltage into three-phase alternating current voltage (consisting of three phases with a 120° offset between phases).

It comes from the association in a bridge of thyristors (or transistor) and diodes. In order to generate sinusoidal currents ia , ib and ic , a two-

by-two complementary operation of the switches K1 K1 ', K2 K2 ' and K3 K3 ' is necessary. And the expression of the sinusoidal currents for a balanced three-phase system is given by the following relation:

$$\begin{cases} i_a = I\sqrt{2}\sin(wt - \varphi) \\ i_b = I\sqrt{2}\sin(wt - \varphi - \frac{2\pi}{3}) \\ i_c = I\sqrt{2}\sin(wt - \varphi - \frac{4\pi}{3}) \end{cases}$$

(16)

w represents the pulsation, I the effective value of the output current and φ the phase shift.

The PWM is used to control the switches of the inverter in order to have sinusoidal current shapes. Thus, its operation consists of control pulses at regular time intervals of variable durations generated and sent to the switches of the inverter.

It is based on the comparison of a reference signal called modulator with amplitude Ar and frequency fr , with a signal called carrier with amplitude Ap and very high frequency fp (modulation frequency). It is characterized by its modulation index m and its voltage adjustment coefficient r all given by the following equation:

$$\begin{cases} m = \frac{f_p}{f_r} \\ r = \frac{A_r}{A_p} \end{cases}$$

(17)

2.3.4 The lead-acid battery

It comes from the association of lead-acid accumulators.

A lead-acid battery consists of a lead oxide (PbO2) cathode and a lead (Pb) anode, immersed in a solution of sulfuric acid. During charging and discharging, the following reversible chemical reaction is obtained:

PbSO2 + Pb + 2H2SO4 ⇌ 2PbSO4 + 2H2O
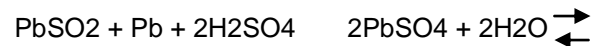
Electrically, the battery can be modeled as a voltage source in series with an internal resistor [15]. Thus, the electrical model equations of the lead-acid battery are given by the following relationship where Qto is the initial charge amount and ηb is the battery efficiency.

$$\begin{cases} V = Eo - r \times i \\ SOC = (Eo - Vd) \times \frac{Cb}{Cn} \\ Eo = [\left(Q_{to} - \int_{to}^{t1} \eta b \times i \times dt\right) \times \frac{1}{Cb}] + Vd \end{cases}$$

(18)

2.3.5 The DC-DC converter

Being a buck converter operating in continuous conduction, its function is to convert the direct voltage of 60 V into a direct voltage of 12V. Its operation is governed by the position of a switch S (closed or open state) [16,17]. Thus, in a first state called ''on state'' where the switch S is closed, the current of the diode is zero and its voltage is negative. The voltage (VL) and the linear variation of the current (ΔI_{L1}) in the impedance L is given by the following equation:

$$\begin{cases} V_L = Vi - Vo = L \times \frac{dI_L}{dt} \\ \Delta I_{L1} = \frac{(Vi-Vo) \times \propto \times T}{L} \\ dVo = \frac{i \times dT}{C} \\ dT1 = \propto \times T = \frac{\propto}{f} \end{cases} \qquad (19)$$

In a second state called ''blocked state'' where the switch S is open, the diode becomes conductive. The voltage (VL) and the variation of the current (ΔI_{L2}) in the inductor become:

$$\begin{cases} V_L = -Vo \\ \Delta I_{L2} = -\frac{Vo \times (T - \propto \times T)}{L} \\ dVo = \frac{i \times dT}{C} \\ dT2 = (1-\propto) \times T = \frac{1-\propto}{f} \end{cases} \qquad (20)$$

In the equations (19) and (20), $\propto$ represents the duty cycle, T the ripple period, L the impedance of the coil, C the capacitance of the capacitor. The expression dVo represents the converter voltage ripple due to imperfections in the output capacitor. The expressions dT represents the duration of a wave cycle when allowance is made for imperfections.

2.3.6 The maximum power point tracking regulator (MPPT)

Its main role is to ensure, with optimal efficiency, the recharging of the batteries through the PV panel. To do this, it continuously optimizes the electrical parameters (voltages, currents) between the PV panel and the battery [18].

The MPPT regulator is actually a boost converter to which the Maximum Power Point Tracking control function is applied.

The operation of the boost converter is almost identical to the DC-DC converter studied above except that it has the function of converting a low DC voltage into a DC voltage of higher value [19].

The control of the Maximum Power Point Tracking is generally carried out electronically, it permanently measures and compares the voltage delivered by the panel with the battery's voltage. Thus, it calculates the maximum power that the PV panel can produce and the maximum power that the battery can receive. From this maximum power, it determines the most suitable voltage for supplying maximum current. This causes the power point it is looking for, be different from the maximum power point of the I(V) characteristic of the panel under STC (Standard Test Condition) test conditions.

There are two methods (algorithms) to provide this maximum power point search function [20].

The method or algorithm for incrementing the inductance consists of a calculation of the derivative of the power of the panel. Thus, this derivative cancels out at the maximum power point, positive to the left of the maximum power point and negative to the right of the maximum power point [21]. However, this method seems more complex because it requires the calculation of several derivatives.

The method or algorithm of disturbance and observation is more widespread in the search for MPP (Maximum Power Point) because it seems easier. It is an algorithm making it possible to find the value of the maximum power point, by measuring the currents and voltages of the PV panel. Thus, it disturbs the value of the voltage of the panel and makes it possible to see each time the impact that it causes on the value of the output power of the panel while having the objective of maximizing the output power without however lowering the output current [22]. It adapts the voltage of the panel each time in order to approach the point of maximum power, without ever reaching it precisely.

2.4 Energy Balance of the SEC Power System

2.4.1 Energy produced

It is made up of two sources of energy production, in particular the storage system and the PV panel, but also has the possibility of receiving energy from the electric motor during the regeneration period. And therefore its energy production must take into account the energy level of the battery pack before driving, the

energy that it could collect or not from the photovoltaic panel and the total energy received during regenerations. We obtain the total energy produced (Ep) as follows:

$$\begin{cases} Ep = Epb + Epp + Epr \\ Epb = Co \times V = Co \times (Eo - r \times I) \\ Epp = \eta \times En \times Sa \\ Epr = \sum P_i \times t_i = \sum U \times I'_i \times \cos\varphi \times t'_i \end{cases} \quad (21)$$

Epb is the energy produced by the battery, Epp is the energy produced by the PV panel, Epr is the energy produced by regeneration, Co is the maximum capacity that the battery can provide, V is the nominal voltage of the storage system , Eo is the no-load voltage of the battery, r is the internal resistance of the battery, η is the yield of the PV panel, En is the solar energy received per m², Sa is the active surface of the panel, P is the power electricity produced by regeneration, t_i' is the maximum duration of regeneration, U is the phase-to-phase voltage of the motor, I' is the current generated during regeneration, $\cos\varphi$ is the phase shift between current and phase of the generator.

2.4.2 Energy consumed

Various energy consumptions are available at almost all levels of the power system. It is therefore necessary to find the energy consumption at the level of the traction system, at the level of the 12V system and even at the level of the PV panel-MPPT regulator-battery system. The energy consumed (Ec) can be calculated as follows:

$$\begin{cases} Ec = EcT + EcA + EcP \\ EcT = (Pu + Pc + Pj + Pconv) \times t \\ P = Pu + Pc = Cm \times \Omega \\ EcA = \eta_{cc} \times \eta_{cab} \times \frac{U'^2}{R} \times t'' \\ EcP = Epp \times (1 - \eta_{reg}) \end{cases} \quad (22)$$

EcT is the energy consumed by the traction system, EcA is the energy consumed by the 12V system, EcP the energy lost between the PV panel and the battery, Pu the useful power delivered by the motor, Pc the constant losses of the motor, Pconv the losses of the reversible converter and of the wiring system of the traction part, P the electromagnetic power of the motor, Cm the electromagnetic torque of the motor, Ω the speed of rotation of the motor, t is the operating time of the motor, η_{cc} is the efficiency of DC-DC converter, η_{cab} is the efficiency of the wiring system of the 12V circuit part, U' is the

12V system voltage, R is the resistance of the 12V circuit appliances, t" is the operating time of the 12V system devices, η_{reg} is the efficiency of the MPPT regulator.

The relation of the useful power of the engine, can be written taking into account the equation of the dynamics of the vehicle. Thus, we have:

$$\begin{cases} Pu = (Cr)_{roues} \times V_{véh} \\ (Cr)_{roues} = (CRR_{moy} \times M \times g + \frac{1}{2} \times \rho \times S_f \times C_x \\ \times V_{véh}^2 + M \times g \times p\% + M\gamma) \times Rr \end{cases} \quad (23)$$

(Cr)wheels the resistive torque applied to the wheels, $V_{véh}$ the speed of the vehicle.

2.4.3 Energy balance

It represents the difference between the vehicle's energy production and consumption. Its expression can therefore be deduced as follows:

$$BE = Ep - Ec \quad (24)$$

2.5 Hypotheses and Simulation Algorithm

2.5.1 Hypotheses

Before starting the calculation of the various electromechanical performances of the vehicle, it is necessary to review certain calculation hypotheses:

➢ A type of rolling is imposed on the vehicle during which there is neither braking nor deceleration producing energy;
➢ The energy input of the capacitors is neglected;
➢ The vehicle is exposed to the sun all day;
➢ The battery pack is fully charged at the start of the experiment;
➢ The internal resistance of the battery pack, as well as the resistance of the motor stator windings being very low so they are neglected;
➢ The iron losses as well as the mechanical losses observable within the motor being very low so they are neglected;
➢ The speed of the vehicle being lower than 50 km/h, then the aerodynamic resistance on this one is neglected.

By taking into account all its hypotheses, the energy balance of the vehicle can be rewritten by the relation (25) and whose numerical resolution makes it possible to calculate the car's range.

$$\begin{cases} BE = Ep - Ec \\ Ep = Co \times V + \Pi \times En \times Sa \\ Ec = (Cm \times \Omega + Pconv) \times t + \Pi_{cc} \times \Pi_{cab} \times \frac{U'^2}{R} \times t'' + \Pi \times En \times Sa \times \left(1 - \Pi_{reg}\right) \\ Cm = (CRR_{moy} \times M \times g + \frac{1}{2} \times \rho \times S_f \times C_x \times V_{véh}^2 + M \times g \times p\% + M\gamma) \times \frac{R_r}{n} \end{cases} \qquad (25)$$
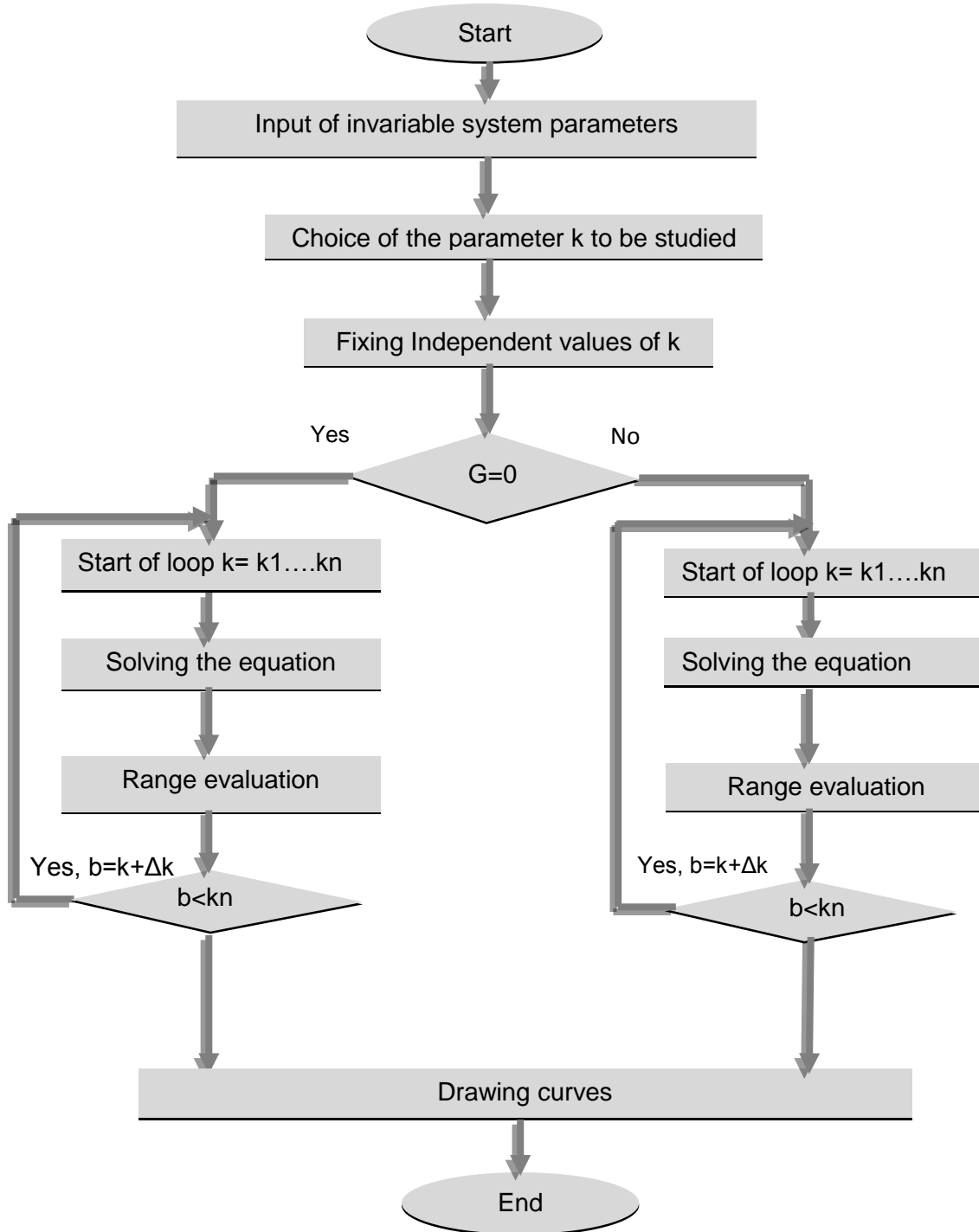

Fig. 4. Simulation algorithm

2.5.2 Simulation algorithm

The algorithm used for the performance evaluation consists, first of all, in fixing the invariable parameters of the system (CRRmoy, g, Sf, Cx, ρ, Pconv, Ŋcc, Ŋcab, U ',Ŋ , Ŋreg, Rr , V , Co, Sa), then to choose a parameter whose evolution considerably influences the range and finally to study the influence of this parameter on the car's range during the existence or not of sunshine. Fig. 4 shows more clearly the different steps of this algorithm.

3. RESULTS AND DISCUSSION

Taking account, the different equations of the relation (25), we evaluate the SEC's range in different conditions using MATLAB's software.

3.1 Solar Radiation

It shows the variation of the intensity of solar radiation during the day used for the simulation (mean day of the month of February). The site considered is Lomé's city in Togo. These global radiation data for each hour of the day were obtained from the European Commission's online software PVGIS.

As shown in Fig. 5, this radiation is weak at the start of the day, gradually increases until it reaches its maximum at noon before gradually decreasing until it disappears at the end of the day. This variation in solar radiation made it possible to evaluate the overall daily sunshine of the day.

3.2 Variation of Thermal Losses in the Thermal Converter

Any increase in the resistive torque of the motor leads to thermal losses within the reversible converter. These heat losses lead to electrical constraints. These electrical constraints have the direct consequence of reducing the range of the vehicle.

3.2.1 Variation of thermal losses according to the car's weight

As shown in Fig. 6, any increase in the mass of the vehicle leads to an increase in heat losses in the reversible converter.

3.2.2 Variation of thermal losses according to the slope

As shown in Fig. 7, the thermal losses within the reversible converter increase considerably as a function of the slope to be crossed by the vehicle.
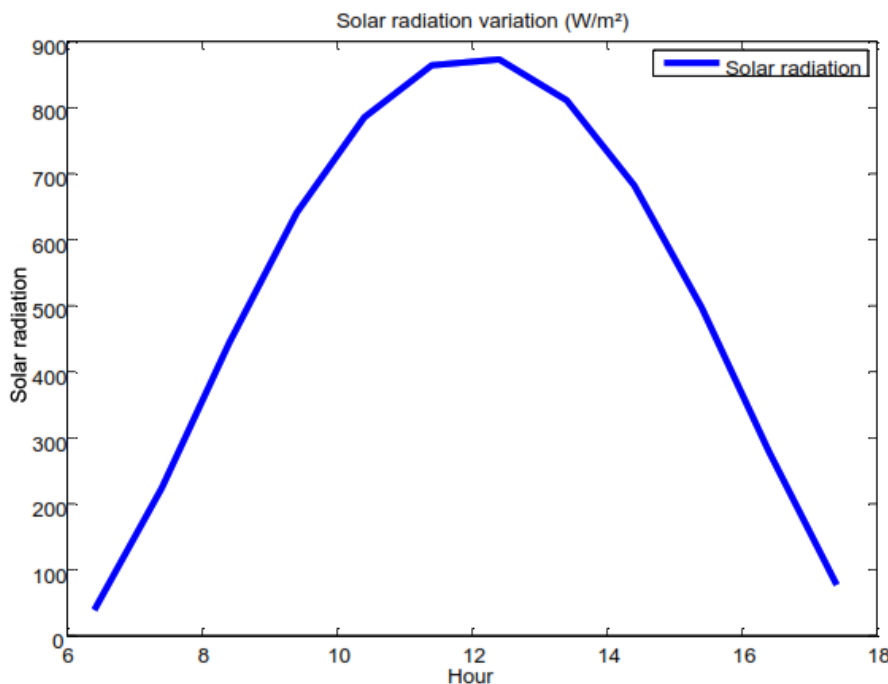

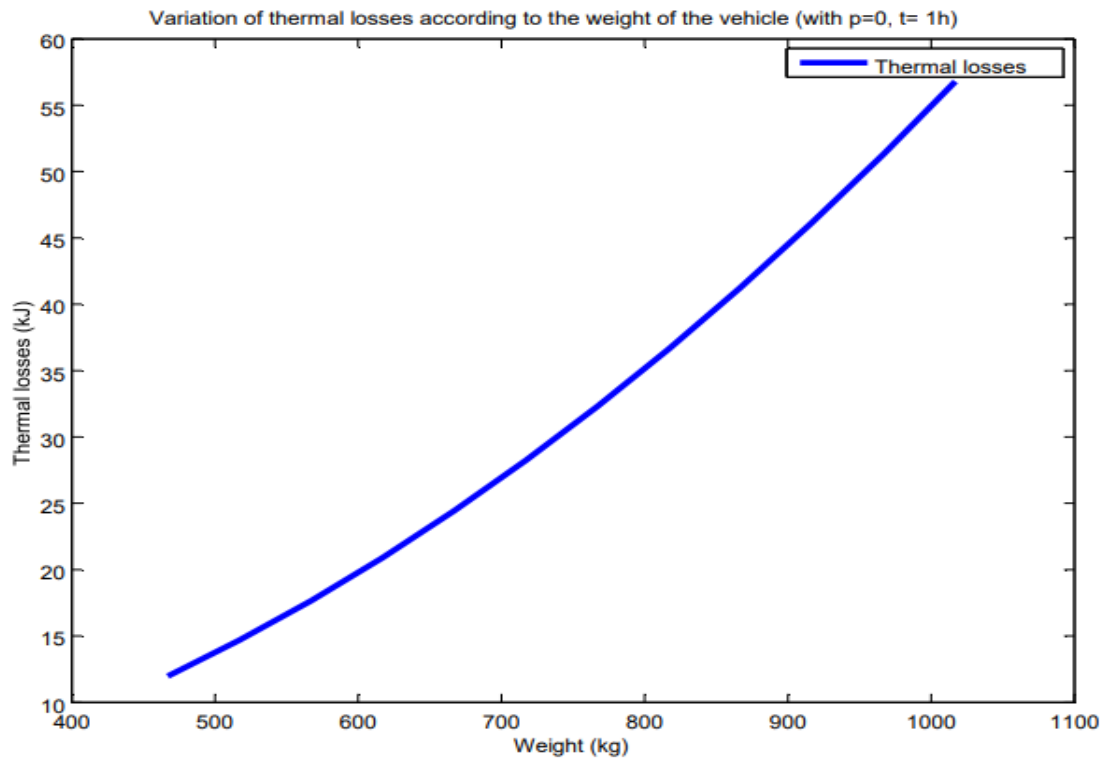**Fig. 5. Variation of solar irradiation as a function of time of day**

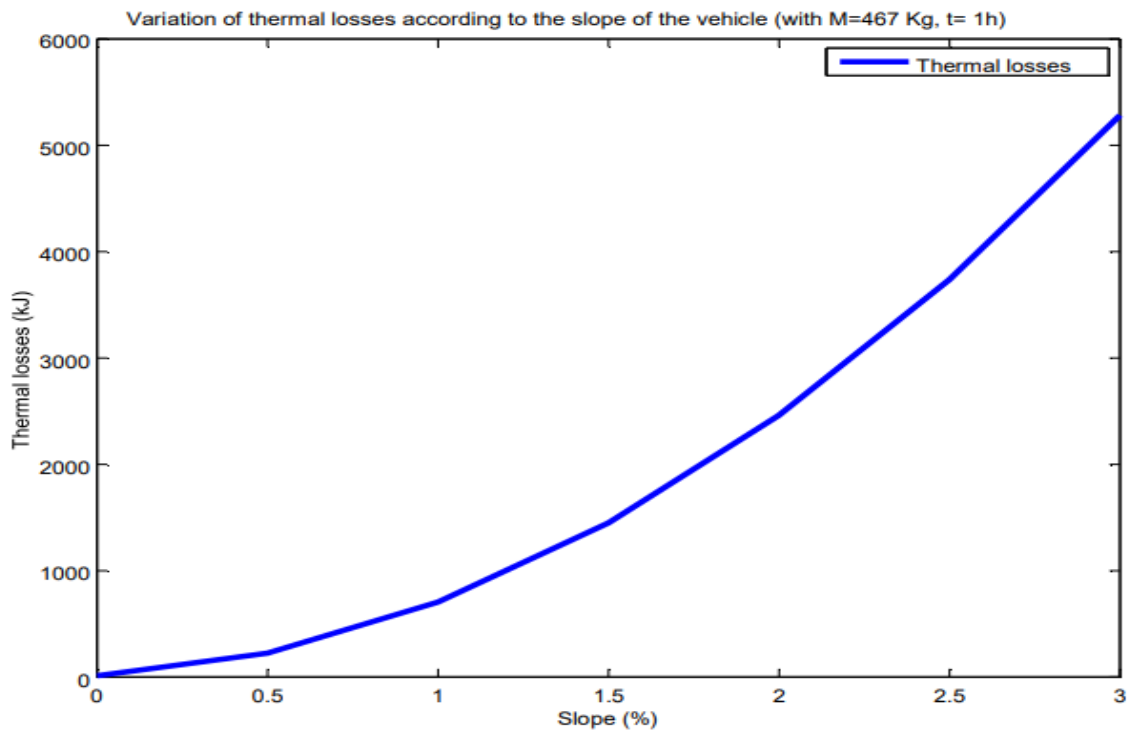**Fig. 6. Variation of thermal losses according to the car's weight**

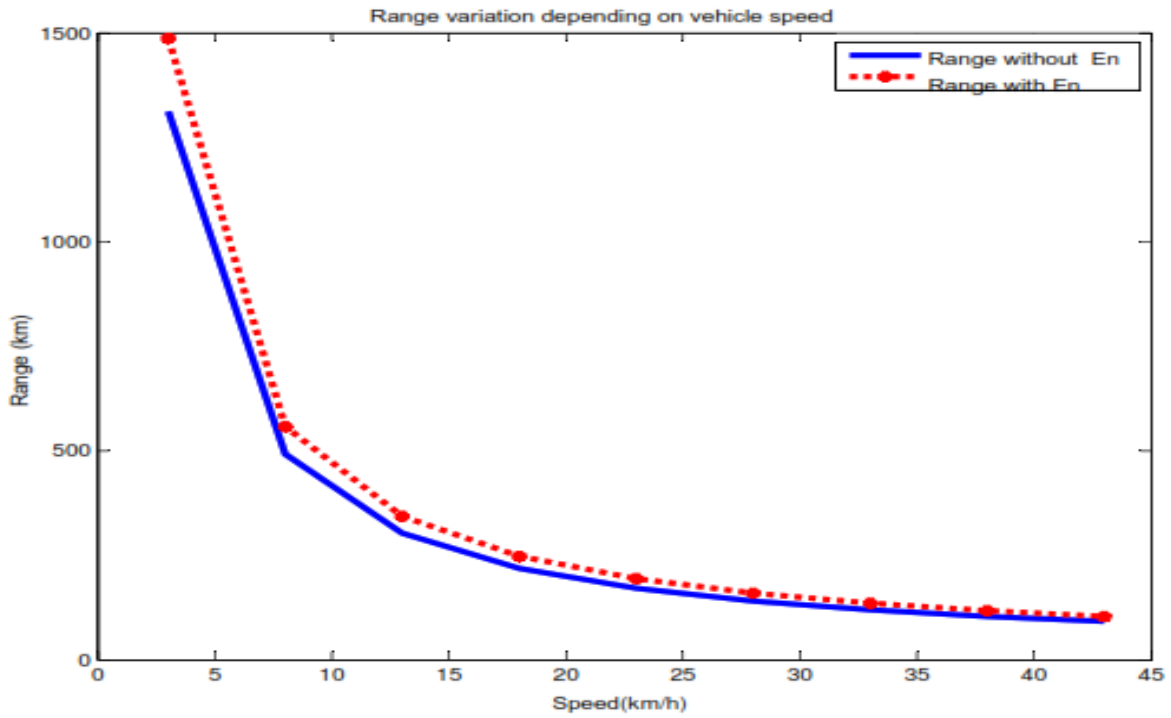**Fig. 7. Variation of thermal losses according to the slope**

Fig. 8. Range variation as a function of car speed
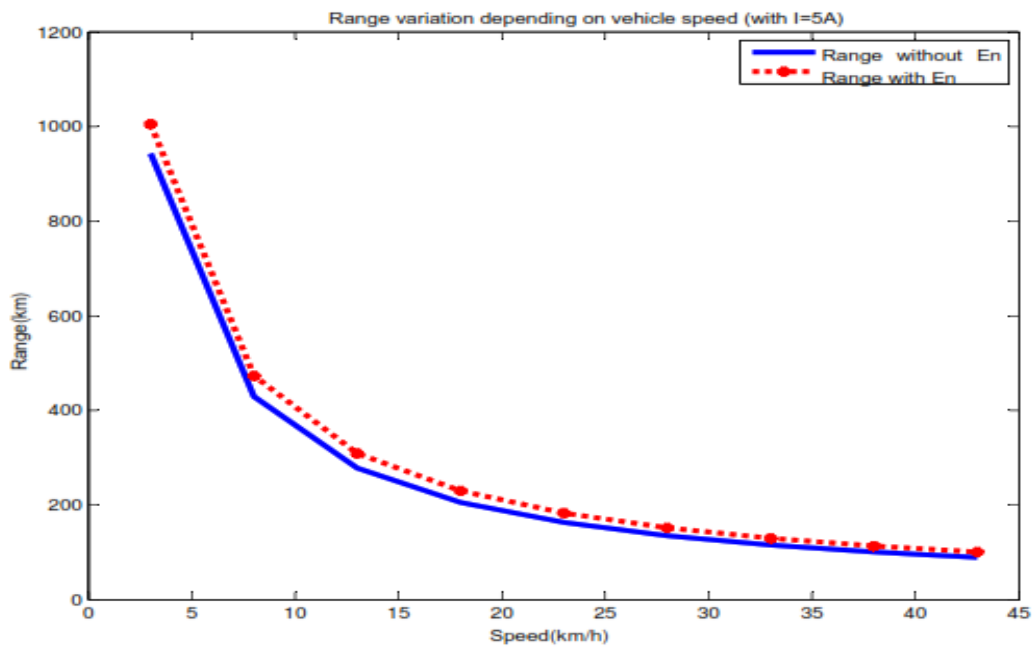

Fig. 9. Range variation as a function of car speed with 5A's loads consumption

3.3 Range Depending on Car's Speed

Fig. 8 illustrates the variation in the range of the vehicle as a function of the vehicle's driving speed during a sunny or non-sunny day. It shows that an increase in the vehicle's driving speed leads to a reduction in the vehicle's range. This range is further extended for a sunny day.

In addition, range decreases more considerably when it is accompanied by a consumption of 12 V circuit devices. This is illustrated in Fig. 9, showing the variation in car's range as a function of vehicle driving speed with constant consumption of 5A current from 12V circuits.
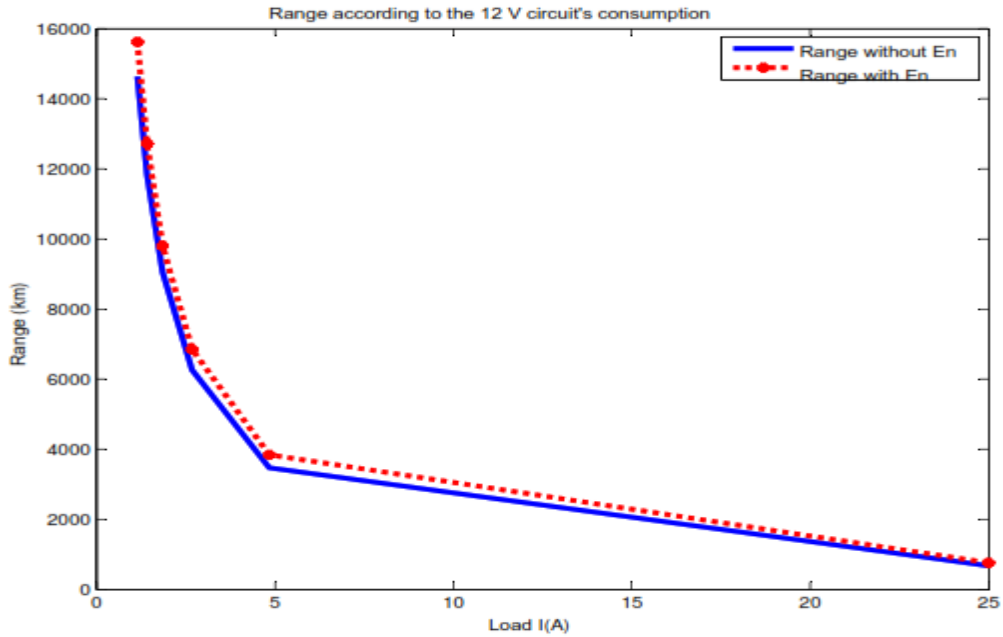

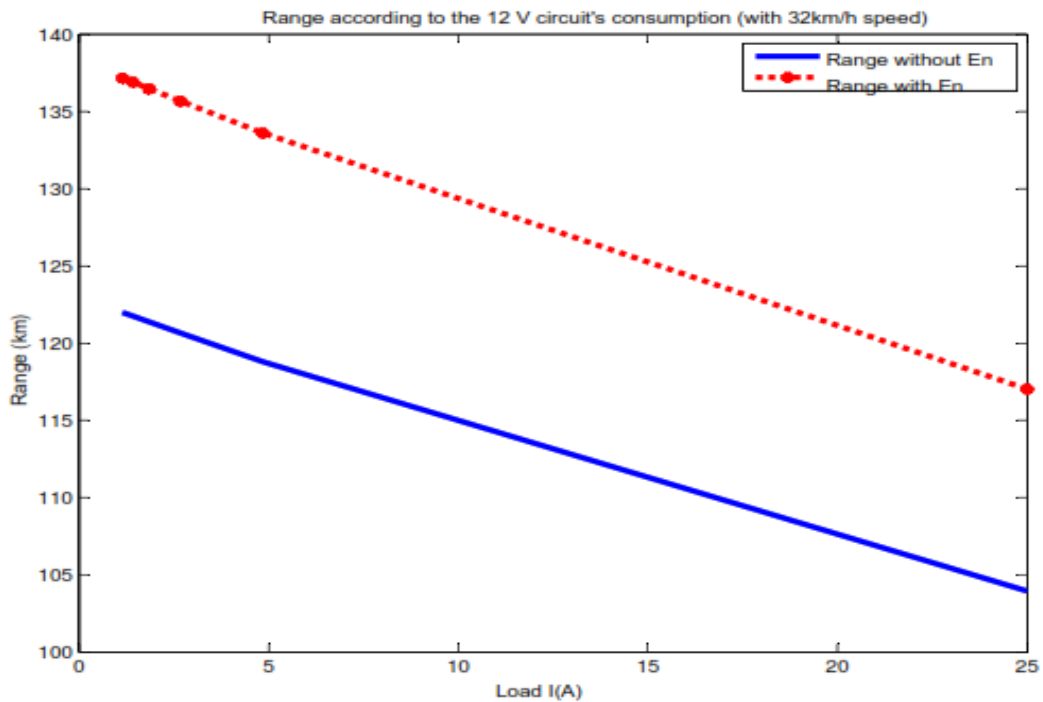**Fig. 10. Range according to the current consumption of 12V devices when the vehicle is stationary**

Fig. 11. Range according to the 12 V devices consumption when the car is traveling at a constant speed of 32 km/h

3.4 Range According to the Consumption of the 12V Circuit

High consumption of 12V devices has a considerable influence on the vehicle's range. And this even when the vehicle is stationary (Fig. 10) or when it is traveling at a constant speed. Nevertheless, an availability of sunshine makes it possible to increase a little more the range of the car as could illustrate it in Fig. 11.

4. CONCLUSION

At the end of our analysis, we obtained results making it possible to understand the car's range variation in various situations taking into account the rolling environment and its internal electrical loads. These results show a considerable decrease in range when the car is confronted with crucial mechanical situations and high energy consumption of the 12 V circuit's devices.

This study therefore provides a general understanding of the behavior of electric vehicles in a sub-Saharan African context. It makes it possible to affirm that the electric vehicle presents very good performance compared to the thermal vehicle for short-distance travel and low driving speeds (as is the case in most African cities).

COMPETING INTERESTS

Authors have declared that no competing interests exist.

REFERENCES

1. International Energy Agency (IEA), Africa Energy Outlook; 2019.
2. SIE-Togo, Rapport 2017; 2017.
3. Ministère des Infrastructures et des Transport, Politique de mobilité et d'accessibilité durable dans les villes togolaises, 2019.
4. Ayetor GK, Quansah DA, Adjei EA. Towards zero vehicle emissions in Africa: a case study of Ghana. Energy Policy. 2020;143:111606.
   DOI:10.1016/j.enpol.2020.111606
5. Collett KA, Hirmer SA, Dalkmann H, Crozier C, Mulugetta Y, McCulloch MD. Can electric vehicles be good for Sub-Saharan Africa? Energy Strategy Rev. 2021;38:100722.
   DOI:1016/J.ESR.2021.100722
6. Booysen MJ, Abraham CJ, Rix AJ, Ndibatya I. Walking on sunshine: pairing electric vehicles with solar energy for sustainable informal public transport in Uganda, Energy Res. Social Sci. 2022;85:102403.
   DOI:10.1016/J.ERSS.2021.102403.
7. Dioha MO, Duan L, Ruggles TH, Bellocchi S, Caldeira K., Exploring the role of electric vehicles in Africa's energy transition: a Nigerian case study. iScience. 2022;Article 103926.
   DOI:10.1016/j.isci.2022.103926.
8. Edwin Solano Araque, Guillaume Colin, Guy-Michel Cloarec, Ahmed Ketfi-Cherif, Yann Chamaillard. Energy analysis of eco-driving maneuvers on electric vehicles. IFAC Papers OnLine. 2018;51–31:195–200.
9. Mruzek M, Gajdáč I, Kučera Ľ, Barta D. Analysis of parameters influencing electric vehicle range, Procedia Eng. 2016;134:165-174.
   DOI:10.1016/j.proeng.2016.01.056.
10. Varga, Bogdan Ovidiu, Arsen Sagoian, Florin Mariasiu. Prediction of electric vehicle range: A comprehensive review of current issues and challenges. Energies. 2019;12(5):946.
    DOI:https://doi.org/10.3390/en12050946.
11. Skuza A, Jurecki RS. IOP Conf. Ser.: Mater. Sci. Eng. 2022;1247:012001.
12. Kanimozhi, Kumar, Harish. Modeling of solar cell under different conditions by Ant Lion Optimizer with Lambert function.
    DOI:10.1016/j.asoc.2018.06.025.
13. Akiyoshi Shimada, Hirohisa Ogawa, Minoru Nakajima. Development of an ultra-thin DC brushless motor for a hybrid car; 2001.
    DOI:10.1016/s0389-4304(01)00114-x.
14. Malinowski, Kazmierkowski, Trzynadlowski. Review and comparative study of control techniques for three-phase PWM rectifiers.
    DOI:10.1016/s0378-4754(03)00081-8.
15. Křivík, Petr. Methods of SoC determination of lead acid battery. Journal of Energy Storage.
    DOI:10.1016/j.est.2017.11.013.
16. Ho-sung Kim, Jong-Hyun Kim, Byung-Duk Min, Dong-Wook Yoo, Hee-Je Kim. A highly efficient PV system using a series connection of DC–DC converter output with a photovoltaic panel.
    DOI:10.1016/j.renene.2009.01.011.

17. Cetin Elmas, Omer Deperlioglu, Hasan Huseyin Sayan. Adaptive fuzzy logic controller for DC–DC converters. DOI:10.1016/j.eswa.2007.11.029.
18. Hua C, Lin J. An on-line MPPT algorithm for rapidly changing illuminations of solar arrays. DOI:10.1016/s0960-1481(02)00214-8.
19. Mukerjee AK, Nivedita Dasgupta. DC power supply used as photovoltaic simulator for testing MPPT algorithms. DOI:10.1016/j.renene.2006.02.010.
20. Yu GJ, Jung YS, Choi JY, Kim GS. A novel two-mode MPPT control algorithm based on comparative study of existing algorithms. DOI:10.1016/j.solener.2003.08.038.
21. Kihal, Abbes, Krim, Fateh, Laib, Abdelbaset, Talbi, Billel, Afghoula, Hamza, An improved MPPT scheme employing adaptive integral derivative sliding mode control for photovoltaic systems under fast irradiation changes. DOI:10.1016/j.isatra.2018.11.020
22. Bounechba, Hadjer, Bouzid, Aissa; Snani, Hamza, Lashab, Abderrazak. Real time simulation of MPPT algorithms for PV energy system. DOI:10.1016/j.ijepes.2016.03.041.

_____